Maximum Achievable Power Conversion Efficiency Obtained Through an Optimized Rectenna Structure for RF Energy Harvesting

Yen-Sheng Chen, *Member, IEEE* and Cheng-Wei Chiu

***Abstract*— High-efficiency rectennas for radio frequency (RF) energy harvesting have been studied for decades, but most of the literature straightforwardly applies the rectenna aiming at dedicated RF sources to this situation, even though the level of input power is significantly different. Since previous studies address antenna design collecting more ambient RF power, the improvement of power conversion efficiency (PCE) has emerged in a scattered way, because the theoretical limit of PCE has not yet been characterized, and the optimal rectenna structure approaching such maximum PCE is still uninvestigated. In this paper, we characterize the performance limit of rectennas with input power ranging from −20 to 0 dBm, proposing optimal rectenna design demonstrating the maximum PCE. The maximum achievable PCE is cast into a mathematical programming problem. Solving this optimization model clarifies the effect of design factors, including operational frequencies, rectifier topologies, and parameterization. To achieve the maximum PCE, our investigation shows that the optimal rectenna structure should not only optimize those design factors but also eliminate the matching circuit between an antenna and a rectifier for ultralow-power scenarios. The resultant PCE at 2.45 GHz is 61.4% and 31.8% at −5 and −15 dBm, respectively, closely approaching the theoretical bound.**

***Index Terms*— Energy harvesting, impedance matching, optimization methods, power transmission, rectennas, rectifiers.**

I. Introduction

ACCORDING to the operational mechanisms and system implementation, wireless power transfer (WPT) is categorized into three techniques: near-field inductive or resonant powering, far-field directive powering, and far-field ambient radio frequency (RF) energy harvesting. Among these techniques, near-field powering has been widely commercialized for supplying energy to portable wireless applications [1]; however, it suffers from extremely short charging distances, limiting the usefulness of WPT, because those devices cannot be fully employed as they are placed above a charging pad. In contrast, far-field directive or ambient powering overcomes this limitation due to the long-distance charging capability; a device can be continuously charged, whenever it is in use or put in a bag. In particular, ambient RF energy harvesting has gathered greater importance over the past few decades, for growing radio transmitters broadcast RF energy around the world. Such ambient energy is regarded as "free" powering sources, making this technology more fascinating than other dedicated WPT; therefore, the focus of WPT puts more and more emphasis on RF energy harvesting, seeking for the efficiency optimization of rectennas with low input power.

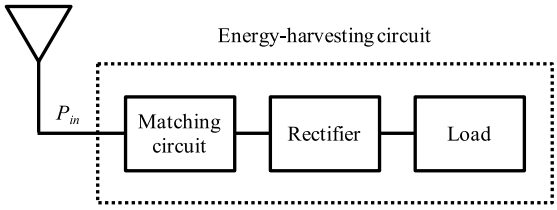

Fig. 1. Block diagram of conventional rectenna structures.

In general, the input power, denoted as P_{in}, for rectennas aiming at RF energy harvesting is lower than 0 dBm [2], which is significantly different than the case of far-field directive powering. Although the level of available RF power is inherently different, most of the literature straightforwardly applies the rectenna aiming at far-field directive powering [2], [3], as shown in Fig. 1, to the applications of RF energy harvesting, lacking investigation on an optimized rectenna structure coping with low-input-power scenarios. More specifically, considering lower input power leads to even lower PCE, recent studies focus on antenna design collecting larger input power, improving the PCE by using broadband antennas [4]–[11], multiband antennas [12]–[25], polarization diversity such as dual-linear polarization [4], [12], [26]–[28], circular polarization [18], [29]–[32], dual-circular polarization [33], [34], and all polarization [35], [36], high-gain antennas [14], [26], [37], [38], combinations of a solar cell and electromagnetic-wave harvesters [39], [40], and multiple elements [5], [41]–[49]; however, although these antenna designs collect more input power to an energy-harvesting circuit, namely, a matching circuit cascaded with a rectifier, few studies have quantified how such energy is consumed in the circuitry. For the aspect of matching circuit, most of the existing studies treat matching components such as inductors, capacitors, or transmission lines as lossless elements; however, as we will see in Section III, even though perfect impedance match is achieved, up to 95% of power may be despoiled by a matching circuit comprising lossy elements in ultralow-power conditions.

Manuscript received November 13, 2016; revised January 30, 2017; accepted March 5, 2017. Date of publication March 14, 2017; date of current version May 3, 2017. This work was supported by the Ministry of Science and Technology, Taiwan, under Contract MOST 105-2221-E-027-016.

The authors are with the Department of Electronic Engineering, National Taipei University of Technology, Taipei 10608, Taiwan (e-mail: yschen@ntut.edu.tw).

Color versions of one or more of the figures in this paper are available online at http://ieeexplore.ieee.org.

Digital Object Identifier 10.1109/TAP.2017.2682228

To date, no research findings have identified such results, and the relation between the lossyness of matching circuits and the level of input power has not yet been fully derived. As for the aspect of rectifier, while many recent studies have proposed improved rectifier design [50]–[60], explicit and systematic design guidelines for optimum rectifier architecture are still critically lacking. These studies enhance the rectifier conversion efficiency by optimizing the signal waveforms [50], [51], selecting optimal RF-dc conversion techniques [52], [53], constructing adaptive rectifier circuits [54], minimizing the sensitivity through resistance compression networks [55], designing a custom IC in a boost converter [56], using a load-modulated two-branch rectifier cooperating with an ultralow-power management unit [57], determining the optimal rectifier topology [58], [59], and optimizing the load conditions [3], [60]. However, the literature puts more emphasis on the characterization of rectifier as $P_{\text{in}} \geq 0$ dBm [3], [59], [60], and it is less clear about how to set every design factor leading to the maximum PCE in energy harvesting applications. Not until the two aspects have clarified do we improve the PCE significantly. Nevertheless, no clear direction has emerged to suggest the optimized rectenna structure aiming at low-input-power scenarios, so the enhancement of PCE has emerged only very slowly and in a more scattered way.

The issue of uninvestigated optimal rectenna structures arises from the fact that the maximum achievable PCE for low-input-power energy harvesting is still largely unknown. Since such a theoretical limit has not yet been characterized, the literature lacks a benchmark to evaluate the performance; accordingly, only relative comparison can be made, so the improvements of PCE are still marginal and limited. Furthermore, due to the lack of the information on maximum achievable PCE, earlier studies are unaware of whether there is redundant circuitry resulting in a poor performance. In fact, in the sphere of near-field WPT, there have been some attempts to establish the maximum achievable PCE, which is the function of design factors such as loaded capacitor, frequency, and coil geometry [61]–[63]; however, to date there has not yet been a study which has systematically determined the theoretical limit of PCE and clarified the optimum level of important design factors for low-input-power far-field WPT.

The purpose of this paper is to develop the maximum achievable PCE over -20 dBm $\leq P_{\text{in}} \leq 0$ dBm and provide guidelines to achieve such a theoretical limit. The established upper bound is the function of design factors including operational frequencies, rectifier topologies, and rectifier parameters. We formulate the maximum achievable PCE as a mathematical programming problem, which can be solved by optimization techniques. The resultant maximum PCE is validated via numerical computation, simulation, and measurement. It is noted that the RF-dc conversion technique is selected as Schottky diodes since they are most often used in rectifiers. Furthermore, we extract the experimental PCE from a large sample of existing rectenna designs based on Schottky diodes [4]–[65] operating in -20 dBm $\leq P_{\text{in}} \leq 0$ dBm, showing that most of rectennas still suffer from insufficient efficiency.

In order to get as close as possible to the theoretical limit, we illustrate the guidelines for setting those design factors to the optimal level. In addition to such optimized rectifier architecture, we further derive the lossyness of matching circuits, which is the function of input power, showing that the additional loss of the matching circuits at $P_{\text{in}} = -20$ dBm runs to 95%, 86%, 65%, and 40% at 900 MHz, 1.8 GHz, 2.4 GHz, and 5.8 GHz, respectively, even though perfect impedance match has been attained. These observations are verified by simulation and measurement, thereby clarifying that a matching circuit between an antenna and a rectifier must be eliminated, for the component losses deteriorate sharply in low-input-power conditions. While some studies have removed a matching circuit and directly matched antenna impedance to rectifier impedance [29], [64]–[66], the intention of this paper is very different from these studies, which aim at applications having larger input power ($P_{\text{in}} \geq 10$ dBm). They have neither observed nor derived the lossyness of matching components for low-input-power scenarios, but for RF energy harvesting reducing the additional loss of a matching network is of utmost importance to improve the overall PCE.

Summarizing the investigation, we propose an optimal rectenna structure closely following the maximum achievable PCE. A fabricated prototype operating at 2.45 GHz exhibits PCE of 61.4%, 50.7%, and 31.8% at -5, -10, and -15 dBm, respectively; these results are very close to the theoretical upper bound, outperforming the PCE reported in the literature. In sum, the significance and novelty of this paper are as follows.

1) We derive the maximum achievable PCE for rectennas with input power ranging from -20 to 0 dBm, providing the performance metrics for rectenna development.
2) From the proposed theoretical limit of PCE, we clarify the effect of related design factors, providing useful guidance for future rectenna designers.
3) We characterize the additional loss of matching circuits, which is the function of input power, showing that the matching circuit must be eliminated for low-input-power energy harvesting.
4) We propose an optimized rectenna structure getting as close as possible to the maximum achievable PCE.

II. Theoretical Limit of Power Conversion Efficiency

The basic structure of a rectenna has been shown in Fig. 1. As the antenna collects RF ambient energy and transmits it to the succeeding circuitry, the matching circuit inserted between the antenna and the rectifier prevents such energy from reflecting or re-radiating from the rectifying circuit. The rectifier consists of diodes, filtering capacitors, and a dc load resistor, converting the incoming RF signals to dc power. During the process of power transferring, the PCE is defined as

$$\eta = \frac{P_{\text{dc}}}{P_{\text{in}}} = \frac{\text{dc output power}}{\text{RF input power}}. \tag{1}$$

where P_{in} is the input RF power collected by the antenna and P_{dc} is the dc power of the load resistor. The PCE not

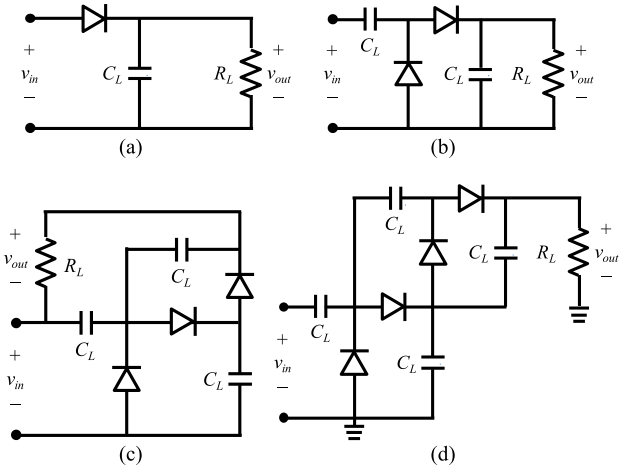

Fig. 2. Various rectifier topologies used in energy harvesting applications. (a) Half-wave rectifier. (b) Single-stage voltage multiplier. (c) Greinacher charge pump. (d) Dickson charge pump.

only characterizes the ability to convert RF power to dc, but it also includes the impedance matching of the energy-harvesting circuit and the insertion loss of the matching circuit.

In order to characterize the maximum achievable PCE, we first consider that the antenna is perfectly matched to the energy-harvesting circuit, and no additional loss occurs in the matching network; therefore, in this situation, the PCE depends on only the rectifier conversion efficiency, which is the function of input power, operational frequency, rectifier topology, and rectifier parameters [2]. The operational frequency considered in this paper includes 900 MHz [9], [10], [12]–[14], [20]–[22], [24], [25], [39], [44], [57], [58], 1.8 GHz [4], [5], [9], [12], [19]–[21], [23]–[25], [39], [54], [61], 2.4 GHz [6]–[8], [12]–[14], [16]–[20], [22]–[27], [29], [32]–[37], [41]–[43], [45], [46], [48], [56], [66], and 5.8 GHz [15], [17], [18], [28], [30], [31], [38], [45], [47], [49], [51]. In addition, the rectifier topologies being investigated are half-wave rectifiers [5], [13], [20], [28], [29], [33], [34], [38], [39], [54], [58], [65], single-stage voltage multipliers [8]–[10], [16], [18], [19], [21], [23], [27], [32], [35], [43], [57], Greinacher charge pumps [7], and Dickson charge pumps [25], [44]; these rectifier topologies are shown in Fig. 2. The rectifying device selected in this paper is the Schottky diode HSMS-286C from Avago.

A. Methodology

We cast the problem of maximum achievable PCE into a mathematical programming model

$$\text{Find } R_L^* \text{ and } C_L^*:$$
$$\max \int_{P_{in,L}}^{P_{in,U}} \eta\,(P_{in},\ f_0,\ R_L,\ C_L)\,dP_{in}$$
$$s.t.\ \begin{cases} -20\ \text{dBm} \le P_{in} \le 0\ \text{dBm} \\ f_0 \in \{900\ \text{MHz},\ 1.8\ \text{GHz},\ 2.4\ \text{GHz},\ 5.8\ \text{GHz}\} \\ 1\ p\text{F} \le C_L \le 100\ p\text{F} \\ 1\ k\Omega \le R_L \le 2000\ k\Omega \end{cases} \tag{2}$$

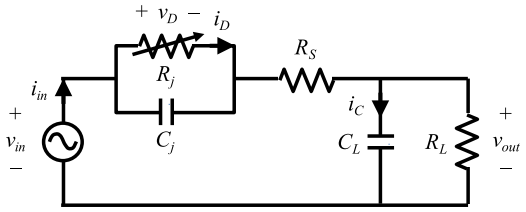

Fig. 3. Equivalent circuit of a half-wave rectifier used for the optimization of the mathematical programming model.

where η denotes the PCE, $P_{\text{in},U}$ and $P_{\text{in},L}$ are the upper and lower bounds of the interested P_{in}, respectively, f_0 is the operational frequency, R_L is the load resistance, and C_L is the filtering capacitance. In this paper, we selected $P_{\text{in},U} = 0$ dBm and $P_{\text{in},L} = -20$ dBm, namely, -20 dBm $\le P_{\text{in}} \le 0$ dBm. The objective function in (2) represents the average PCE over the interested region, and solving such a model provides the optimal parameters for R_L and C_L with respect to given P_{in} and f_0.

The mathematical programming model (2) can be solved by optimization techniques. As the structural analysis tool is Agilent Technologies' advanced design system (ADS) circuit simulation software, the optimization algorithm dealing with (2) is the enumeration method. To unite the two modules in one platform, we used MATLAB as the control and optimization compiler, thereby determining the maximum PCE. Furthermore, in order to verify the optimal solution, we also derived the expression of η and applied numerical optimization to this model. More specifically, the equivalent circuit for the half-wave rectifier is depicted in Fig. 3. The Schottky diode comprises a nonlinear resistor R_j characterized by the $I-V$ relation of a diode at dc, a series resistor R_S, and a junction capacitor C_j. The equivalent circuit parameters of the Schottky diode used are $R_S = 6.0\ \Omega$, $C_j = 0.18$ pF, and $R_j = 8.33 \times 10^{-5} \times n \times T/(i_b + I_s)$, where i_b is the externally applied bias current, I_s is the saturation current ($I_s = 5 \times 10^{-8}$ A), n is the ideality factor ($n = 1.08$), and T is the room temperature. Additionally, the following expressions are derived with two assumptions, including that the voltage drop across the input port of the rectifier consists of only the fundamental-frequency term and the junction capacitance C_j is constant.

Consider a voltage source $v_{\text{in}} = V_m \cos(\omega t)$ applied to the input port of the rectifier. The voltage drops across the loop can be expressed by using Kirchoff's voltage law, and the currents flowing into node N are subjected to Kirchoff's current law. Additionally, based on the component model of the diode, the current i_D can be expresses as

$$i_D = I_S \times \left[\exp\left(\frac{v_D}{nV_T}\right) - 1\right] \tag{3}$$

where v_D is the voltage drop across R_j and V_T is the turn-ON voltage of the Schottky diode ($V_T = 0.026$ V at room temperature for HSMS-286C).

These expressions lead to a simultaneous differential equation for v_{out}, namely, the output voltage on R_L. However, to determine the closed-form expression of v_{out} from the simultaneous differential equation is difficult. Therefore, we

TABLE I
OPTIMAL PARAMETERS FOR DIFFERENT RECTIFIER TOPOLOGIES

Rectifier topology		900 MHz	1.8 GHz	2.4 GHz	5.8 GHz
Half-wave rectifier	R_L^*	73 kΩ	27 kΩ	10 kΩ	2 kΩ
	C_L^*	10 pF	10 pF	10 pF	10 pF
Single-stage voltage multiplier	R_L^*	292 kΩ	108 kΩ	40 kΩ	8 kΩ
	C_L^*	10 pF	10 pF	10 pF	10 pF
Greinacher charge pump	R_L^*	657 kΩ	243 kΩ	90 kΩ	18 kΩ
	C_L^*	10 pF	10 pF	10 pF	10 pF
Dickson charge pump	R_L^*	1168 kΩ	432 kΩ	160 kΩ	32 kΩ
	C_L^*	15 pF	15 pF	15 pF	15 pF

apply the Euler method [67], a numerical procedure for solving simultaneous differential equations with given initial values, to this situation. Once v_{out} is solved, the numerator of η, namely, P_{dc} can be calculated by

$$P_{\text{dc}} = \frac{\left(\frac{1}{T}\int_0^T v_{\text{out}}(t)dt\right)^2}{R_L} \tag{4}$$

where T is the reciprocal of the operational frequency.

On the other hand, the denominator of η, namely, the average power P_{in}, can be computed from the voltage and current of the voltage source. We expand the current i_{in} by the Fourier series representations, using the orthogonal properties for trigonometric functions to calculate P_{in}. As P_{in} and P_{dc} are obtained, the efficiency η can be determined by using (1). However, once the magnitude of the diode reverse voltage $-v_D$ is larger than the breakdown voltage of the diode, denoted as v_{br}, the output voltage v_{out} remains constant, and so does the output power P_{dc}. In this case, v_{out} is equal to half the breakdown voltage ($v_{\text{br}} = 7$ V for HSMS-286C), despite the increasing level of the input power P_{in}. Accordingly, the efficiency calculated by the following equation decreases:

$$\eta(-v_D \geq v_{\text{br}}) = \frac{v_{\text{br}}^2/4R_L}{P_{\text{in}}}. \tag{5}$$

Finally, with the numerical expression η, the constrained programming problem (2) can be solved by optimization techniques, such as shotgun hill climbing [68]. The overall numerical process, including the procedure for computing η and the succeeding optimization, is developed into one single platform compiled by using MATLAB.

B. Results and Discussion

The optimum solutions for each rectifier topology at the targeted frequency are listed in Table I. The associated maximum PCE at various frequencies is shown in Fig. 4. These results can clarify the effect of design factors. First, although multiple-stage rectifiers provide larger output voltage, the half-wave rectifier exhibits the maximum PCE, whatever the operational frequency is. This observation indicates that reducing the number of diodes and filtering capacitors used leads to higher PCE, clarifying that minimizing the component loss for low-input-power situations is important.

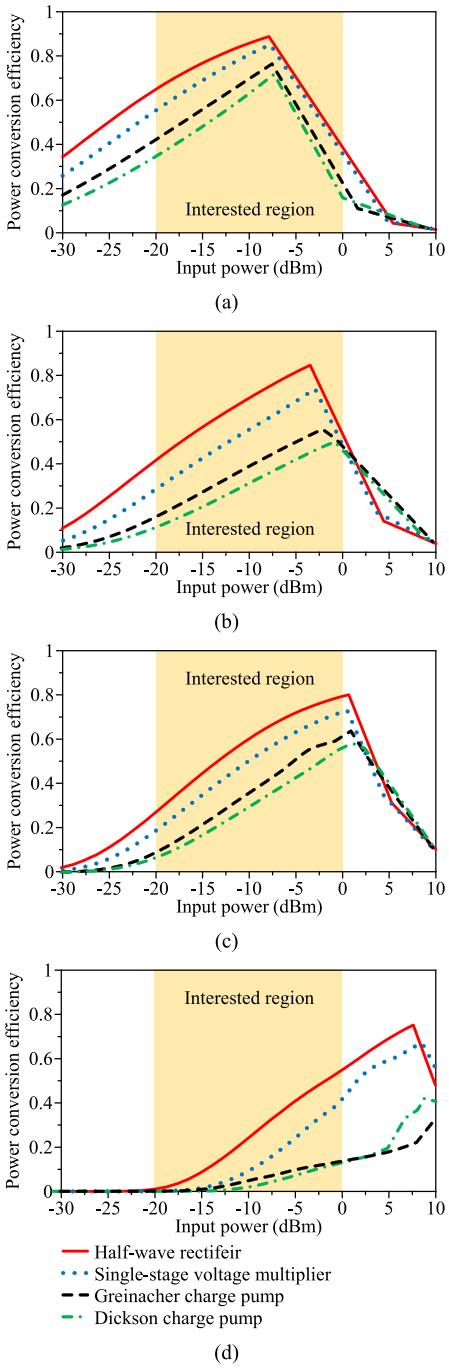

Fig. 4. Maximum achievable PCE resulting from different rectifier topologies at (a) 900 MHz, (b) 1.8 GHz, (c) 2.4 GHz, and (d) 5.8 GHz.

Second, over the interested range of input power, the frequency leading to the maximum average efficiency is 900 MHz. The effect of operational frequencies is illustrated in Fig. 5, which demonstrates that harvesting ambient 900-MHz energy yields higher average PCE. However, the selection of operational frequency involves more aspects apart from pursuing the maximum efficiency, for the ambient energy at that frequency must exhibit sufficient power density. In addition, Fig. 5 indicates that optimal input power exists for each operational frequency. Such optimal input power can be obtained if the magnitude of the reverse voltage on the diode is equal to its breakdown voltage. For the diode used,

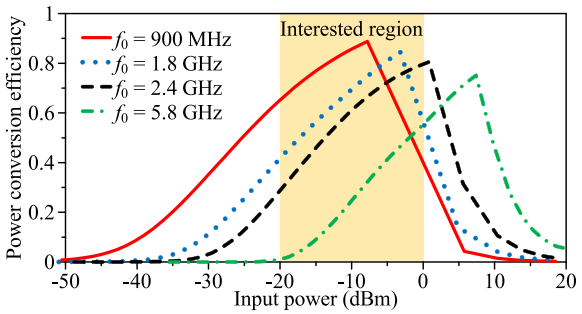

Fig. 5. Maximum achievable PCE resulting from different operational frequencies.

the optimal input power resulting in the maximum PCE at 900 MHz, 1.8 GHz, 2.4 GHz, and 5.8 GHz is −7.8, −3.2, 0.8, and 7.4 dBm, respectively. The trend suggests that the higher the operational frequency the larger the optimal input power is.

Lastly, our sensitivity analysis shows that optimal parameterization for R_L and C_L is crucial for rectenna design. Although the PCE is relatively insensitive to the change of C_L, it is imperative to determine the optimal R_L so that the PCE is maximized. Except for the optimal R_L shown in Table I, larger or smaller load resistances result in worse PCE. In addition, Table I suggests that a larger load resistance is required for a lower operational frequency. Such an observation can be explained by the relation between the operational frequency and the parallel connection of C_j and R_j. As the operational frequency increases, the junction capacitance C_j exhibits smaller impedance, and so does the parallel-connected impedance of C_j and R_j. In order to keep the same magnitude of the maximum output voltage, which satisfies a voltage divider formed with R_L and the parallel-connected impedance of C_j and R_j [69], this output voltage will require a smaller R_L for a higher frequency. In sum, the rectifier load, which may consist of a power management unit and a device, should be carefully designed so that they achieve the optimal parameterization.

In order to verify the proposed maximum achievable PCE, the optimal rectifier architecture, namely, the half-wave rectifier with the optimal load, is fabricated and tested. In this case, only the rectifier conversion efficiency is measured; neither matching networks nor antennas are connected. Such measured rectifier conversion efficiency is shown in Fig. 6. Additionally, the maximum PCE determined by the numerical optimization is also shown and compared in Fig. 6. The simulated results, the numerically computed ones, and the measured curves agree well for all the operational frequencies.

The results shown in Fig. 6 can be understood as the theoretical limit of average PCE for the input power ranging from −20 to 0 dBm. To further validate this statement, Fig. 6 also shows a survey of the state-of-the-art PCE for energy harvesting applications [4]–[65]. We plot and compare the experimental PCE in the literature to the derived theoretical upper bound. Many of the existing designs have a suboptimal performance, and they could have been predicted to perform poorly if the proposed design guidelines were more clearly understood from the start. In addition, the PCE of some

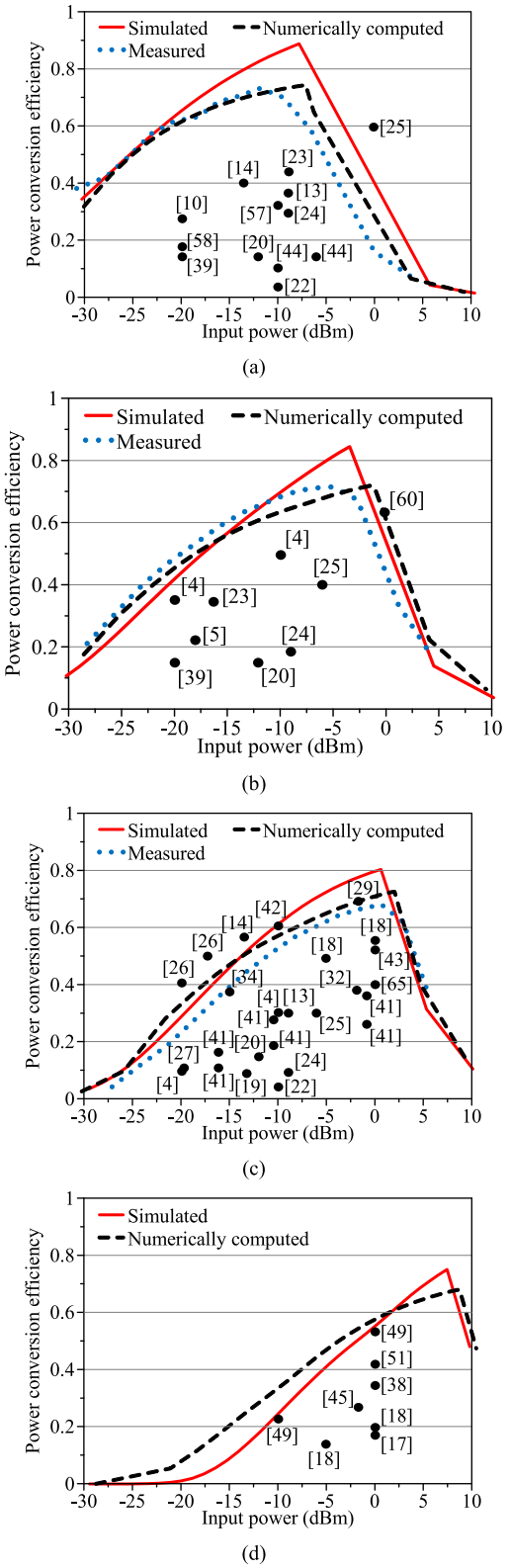

Fig. 6. Simulated, measured, and numerically computed maximum achievable PCE, compared to the experimental results published in the literature. (a) 900 MHz. (b) 1.8 GHz. (c) 2.4 GHz. (d) 5.8 GHz.

rectenna designs exceeds the proposed theoretical limit [14], [25], [26], [42]; several of the reasons are as follows. First, the proposed theoretical limit aims at the maximum of average PCE over −20 dBm $\leq P_{\text{in}} \leq$ 0 dBm. If a rectenna is

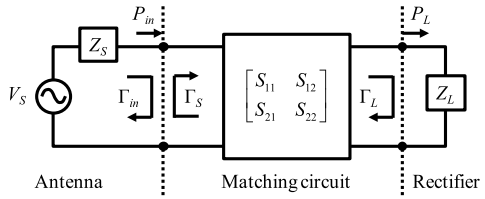

Fig. 7. Schematic of a matching circuit with an antenna and a rectifier.

devoted to only one single input power, such as 0 dBm [25], −18 dBm [26], and −15 dBm [14], these rectennas may show superior efficiency. Second, the optimized results are evaluated using the Schottky diode HSMS-286C. The rectennas having higher efficiency may use diodes with extraordinary specifications, such as a smaller series resistance R_S, a larger breakdown voltage $v_{\rm br}$, a smaller junction capacitance C_j, or a smaller turn-ON voltage V_T. Lastly, the performance of these rectennas may be overestimated by ignoring losses or measurement error. Nevertheless, the proposed upper bound of PCE is valid for most of the cases, thereby providing the benchmark of performance claims for rectenna engineers.

Upon examining the existing rectenna designs for energy harvesting applications, a more crucial issue, excepting optimized rectifier architecture, must be carefully addressed. The so-called maximum achievable PCE in this section is provided by neglecting the return loss of input power and the insertion loss of a matching network. While a matching circuit must be introduced in order to maximize the return loss reaching the antenna, it is desired to minimize the additional loss of the matching circuit so that the theoretical limit proposed in this section can be achieved. Conventionally, the literature is used to regarding the matching circuit as lossless networks. Once a rectenna performs poorly, the underlying reason has seldom been attributed to the lossyness of the matching circuit. However, we have already seen that minimized component loss is so important that rectifiers with more number of diodes and filtering capacitors lead to unacceptable PCE. This further indicates that the maximum PCE cannot be obtained until the lossyness of the matching circuit is fully characterized. In the next section, we will derive the relation between the lossyness of matching circuits and the level of input power, showing that an optimal rectenna structure should not only optimize the rectifier design, but it must eliminate the matching circuit in low-input-power conditions.

III. Characterization of the Lossyness of Matching Networks

Consider a matching circuit connected to an antenna and a rectifier, respectively, as shown in Fig. 7. The additional loss of the matching circuit is characterized by the ratio of power transmitted to the rectifier to the input of the matching network, which can be expressed as the operating power gain G_p given by [70]

$$G_p = \frac{P_L}{P_{in}} = \frac{1}{1-|\Gamma_{in}|^2}|S_{21}|^2\frac{1-|\Gamma_L|^2}{|1-S_{22}\Gamma_L|} \tag{6}$$

where $P_{\rm in}$ is again the input power to the matching circuit, P_L is the power delivered to the rectifier, the input impedance

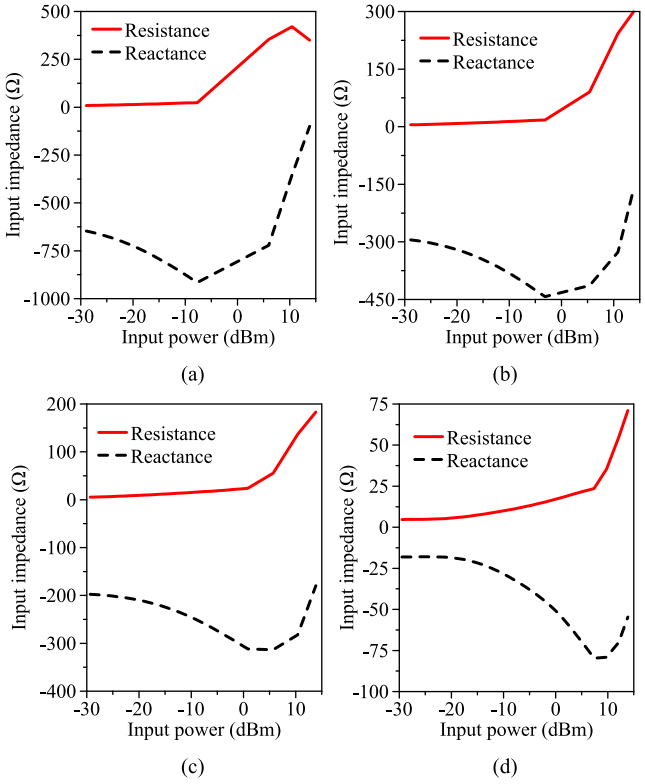

Fig. 8. Input impedance of different optimal rectifier designs. (a) 900 MHz. (b) 1.8 GHz. (c) 2.4 GHz. (d) 5.8 GHz.

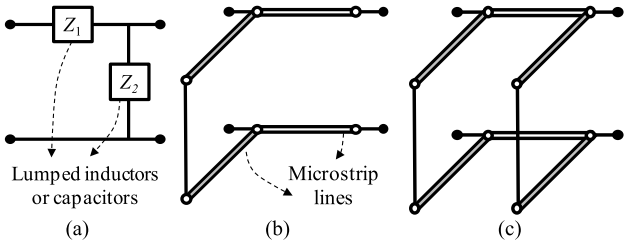

Fig. 9. Schematic of different matching techniques. (a) *LC* matching network. (b) Single-stub impedance tuner. (c) Double-stub impedance tuner.

of which is denoted as Z_L, $\Gamma_{\rm in}$ is the input reflection coefficient when the matching circuit is cascaded with the rectifier, Γ_L is the reflection coefficient of the matching circuit looking into the rectifier, and S_{mn} is the scattering parameter of the matching circuit. In particular, the input impedance of the optimal rectifier serving each frequency is shown in Fig. 8.

Common matching circuits applied to rectenna applications include *LC* networks [7], [10], [12], [16], [22], [24], [27], [36], [37], [44], [54], single-stub tuners [23], [35], [42], [57], and double-stub tuners [5], [14], [18], [19], [28], [57], [66], as shown in Fig. 9. For each operational frequency considered, these matching techniques are, respectively, applied to the load impedance at $P_{\rm in} = -10$ dBm. The design goal of these matching circuits is to minimize $|\Gamma_{\rm in}|$. In ADS simulation, the *LC* networks are modeled by using Murata capacitors (GRM 15 series) and inductors (LQP 15M series). Additionally, the transmission-line-based techniques are constructed by using microstrip lines fabricated on either

TABLE II
SCATTERING PARAMETERS OF THE MATCHING CIRCUITS AT 2.4 GHz

Matching circuit	S_{11}	S_{12}	S_{21}	S_{22}
LC network (simulated)	0.96∠−18°	0.29∠93°	0.29∠93°	0.93∠24°
FR4 single-stub tuner (simulated)	0.94∠50°	0.29∠−54°	0.29∠−54°	0.93∠24°
FR4 double-stub tuner (simulated)	0.93∠36°	0.31∠−61°	0.31∠−61°	0.92∠25°
RO 5880 single-stub tuner (simulated)	0.97∠65°	0.22∠−46°	0.22∠−46°	0.97∠23°
RO 5880 double-stub tuner (simulated)	0.97∠60°	0.22∠−48°	0.22∠−48°	0.97∠23°
FR4 single-stub tuner (measured)	0.95∠104°	0.28∠−22°	0.28∠−22°	0.94∠33°
FR4 double-stub tuner (measured)	0.95∠95°	0.30∠−27°	0.30∠−27°	0.93∠33°

FR4 (dielectric constant $\varepsilon_r = 4.4$ and loss tangent $\tan\delta = 0.02$) or Rogers Corp. Duroid 5880 ($\varepsilon_r = 2.2$ and $\tan\delta = 0.0004$) substrates. After optimizing the design parameters, the resultant return loss is larger than 20 dB at $P_{\text{in}} = -10$ dBm, whatever matching techniques are applied. In addition, the single-stub and double-stub tuners constructed on FR4 are fabricated, and the measured results also indicate that excellent impedance matching has been achieved.

However, as the operating power gain is observed, the power delivered to the rectifier is surprisingly low. Substituting the scattering parameters of each matching circuit Γ_{in} and Γ_L into (6), the simulated and measured G_p are shown in Fig. 10. In particular, the scattering parameters of the matching circuits at 2.4 GHz are listed in Table II. Fig. 10 shows good agreement between simulation and measurement. These results indicate that G_p varies from the level of input power. At 900 MHz, less than 10% of power is transferred to the rectifier if *LC* networks or transmission-line-based impedance tuners fabricated on FR4 are used. Only when the input power is larger than 10 dBm can energy successfully transmit to the rectifier. Besides, even though a less lossy substrate (Duroid 5880) is used, in the interested power region more than 65% of power is dissipated due to the loss of the matching circuits.

Similar results can be observed as operating the rectennas at 1.8 or 2.4 GHz. If *LC* networks or transmission-line-based impedance tuners fabricated on FR4 are used, over 50% of power is consumed by the lossy elements of the matching networks. Such additional loss cannot be reduced unless Duroid 5880 is applied; nevertheless, as well-known, the cost of Duroid 5880 is much higher, so a number of studies concerning energy-harvesting applications still use FR4 as the substrate [4], [7], [9], [10], [20], [32], [35], [37], [43], [48], [65]. In this way, the upper bound of PCE derived in Section II is impossible to be obtained, for more than half available power is lost. Only the 5.8-GHz matching circuits provide slight loss; however, the rectifier conversion efficiency has the poorest performance at this frequency, as already shown in Fig. 5.

From these observations, we can point out important features characterizing matching networks in low-input-power conditions. Although G_p inherently is not the function of input power, G_p is dependent on Γ_L and Z_L. Consider the *LC* network and the single-stub tuners fabricated on FR4/Duroid 5880, all at 2.4 GHz. Fig. 11 shows their contour plots of G_p, versus load resistance R_L and load reactance X_L. It can be seen that the *LC* network and the single-stub tuner fabricated on FR4 exhibit similar level curves, but the single-stub tuner constructed on Duroid 5880 shows a larger area

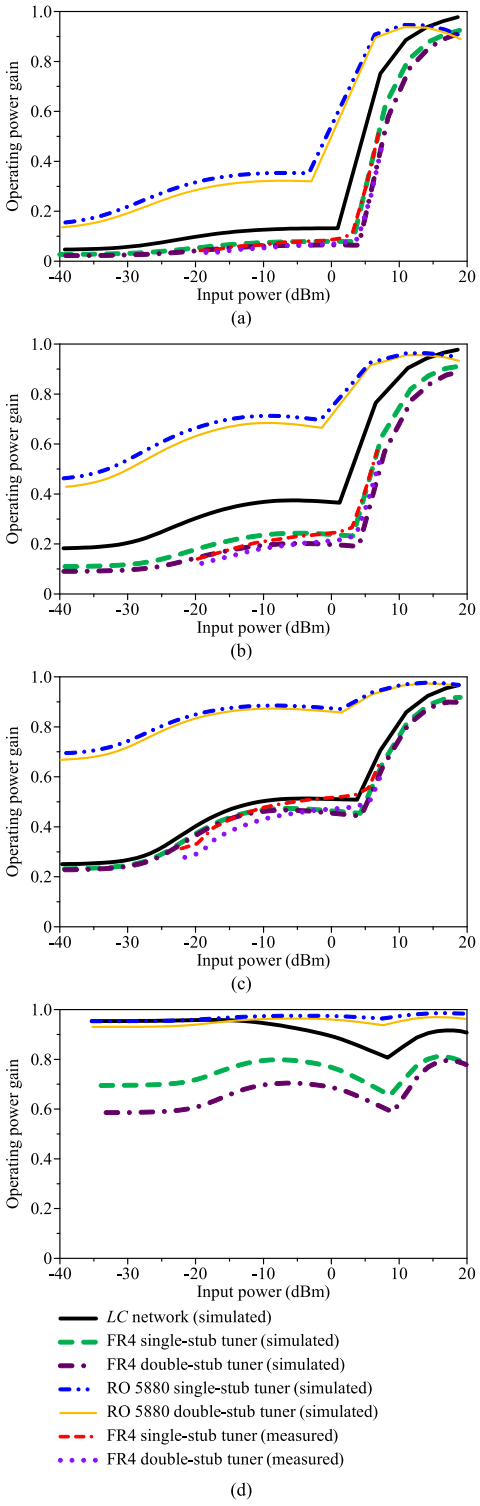

Fig. 10. Operating power gain of matching networks designed by various techniques. (a) 900 MHz. (b) 1.8 GHz. (c) 2.4 GHz. (d) 5.8 GHz.

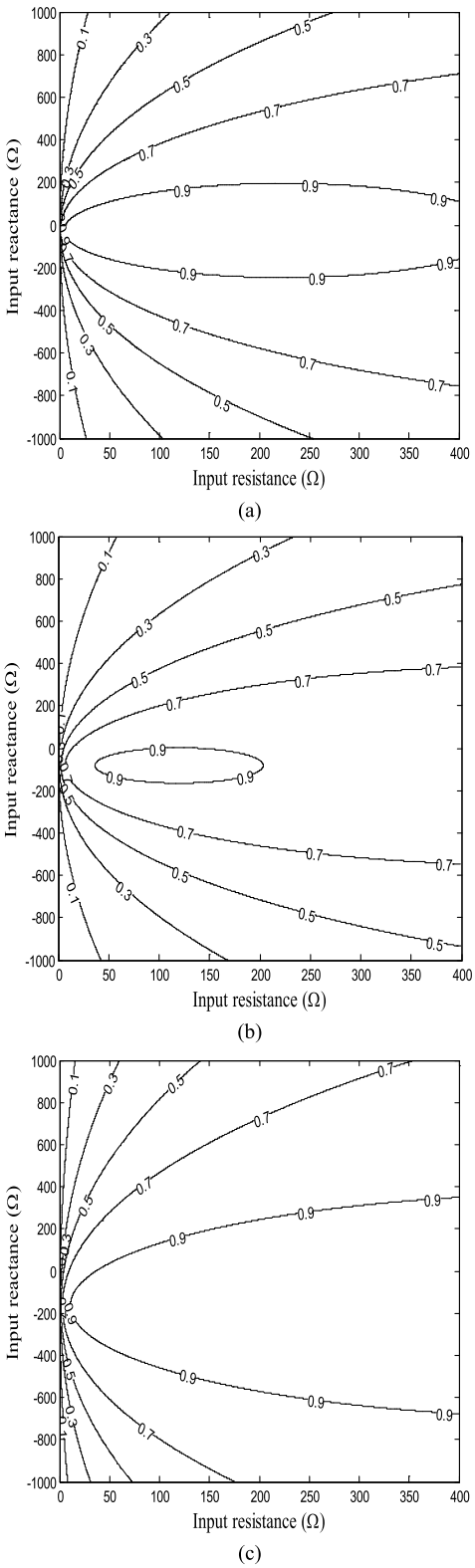

Fig. 11. Contour plot of operating power gain for (a) *LC* network, (b) single-stub tuner fabricated on FR4, and (c) single-stub tuner fabricated on Duroid 5880. Operational frequency: 2.4 GHz.

having greater G_p. Only lossless matching networks provide $G_p = 1$ (or $G_p = 0$ dB) everywhere; once a matching circuit is constructed by lossy elements, no matter how lossy they are, the curves of other G_p levels appear. Besides, the "sweet spot" of the contour plot is the area having small $|X_L|$ and large R_L. However, the load reactance over -20 dBm $\leq P_{\text{in}} \leq 0$ dBm is highly capacitive, and the load resistance is very small ($0\ \Omega \leq R_L \leq 30\ \Omega$), as shown in Fig. 8(c). This brings G_p in this case to move away from the "sweet spot" of the contour, thereby decreasing the output power to the rectifier. In contrast, for large-input-power scenarios such as $P_{\text{in}} \geq 5$ dBm, the input resistance of the rectifier is comparatively large ($30\ \Omega \leq R_L \leq 400\ \Omega$), so the corresponding G_p is satisfactory. Since earlier studies put more emphasis on the rectennas having large input power [3], the lossyness of matching networks has not been given the attention it needs. However, once RF ambient energy harvesting is pursued, the additional loss of matching circuits becomes significant, and it must be carefully addressed.

On the other hand, although the investigation of rectifier conversion efficiency shows that 900-MHz rectifiers have largest average PCE over -20 dBm $\leq P_{\text{in}} \leq 0$ dBm, yet the matching circuits have largest additional loss. In contrast, the matching circuits serving 5.8 GHz are approximately lossless, but the rectifier conversion efficiency is totally unacceptable for low-input-power harvesting. This further poses a dilemma for selecting an operational frequency. To compromise between the rectifier conversion efficiency and the operating power gain of matching circuits, 2.4-GHz rectennas thus become the most popular choice.

In sum, while it may be straightforward that inserting a matching circuit leads to additional loss, the literature is used to treat such loss as acceptable or imperceptible. However, after characterizing the lossyness, which runs to 95% in the worst case, the overall PCE may be more adversely affected by the matching circuit than by the rectifier design. The results shown in this section clarify the limitation of conventional rectenna structures, indicating that the matching circuit must be eliminated for low-input-power rectenna applications.

IV. Optimized Rectenna Design

Although the PCE defined in this paper (1) does not include the radiation efficiency of an antenna, in this section we will first propose a high-efficiency antenna to enhance the overall performance. Afterward, the proposed optimal rectenna structure will be validated experimentally.

A. Antenna Configuration

Conventionally, patch antennas have been applied to the antenna element that directly conjugate matches to the rectifier impedance [29], [64]–[66]. However, patch antennas may have poor radiation efficiency if the associated impedance is highly inductive. This effect is particularly serious once the metal patch is fabricated on relatively lossy substrates, such as FR4. Therefore, a more suitable antenna configuration for the purpose of directly conjugate match is highly demanded.

This design goal is basically similar to the tag antenna design for RF identification. While the literature is full of discussion on using patch antennas [15], [23], [25], [27]–[38], [42], [43], [45]–[49], [56], [61], [64]–[66], dipole antennas, loop antennas, or quasi-Yagi antennas [5], [14], we bring the inductively coupled feeding structure [71] to the antenna

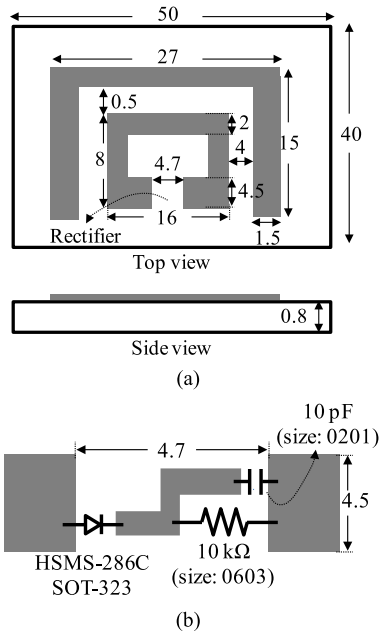

Fig. 12. (a) Configuration of the optimized rectenna structure and (b) closer look at the rectifier, directly mounted to the inductively coupled-feed loop (unit: mm).

element for RF energy harvesting. Fig. 12 shows the proposed antenna configuration, consisting of a meandered dipole antenna, serving as the radiating body, and a rectangular loop, to which the rectifier circuit will be mounted. In the following demonstration, the operational frequency is set to 2.45 GHz, and the substrate used is a 0.8-mm-thick FR4. The rectifier circuit is the optimal half-wave rectifier with a complex impedance $6 - j170\ \Omega$ at$P_{\text{in}} = -10$ dBm. Therefore, the design goal of the antenna is to achieve a complex input impedance $6 + j170\ \Omega$ at the feeding port. Since the geometry of rectangular loop and that of the meandered dipole can be designed separately [71], the geometric parameters of the rectangular loop is first tuned to have an input impedance of $j170\ \Omega$, which can compensate for the capacitive component of the rectifier reactance. Subsequently, the geometry of the radiating body, whose initial dimension is set to half wavelength, is tuned to match the rectifier resistance, namely, 6 Ω.

To facilitate assessing the performance of the proposed inductively coupled-feed antenna, two conventional antennas of the same operational frequency are also designed on the same dielectric substrate. These conventional designs include a patch antenna and a quasi-Yagi antenna, as shown in Fig. 13. Their impedance is designed to be conjugate matched to the input impedance of the same optimal rectifier. The complex reflection coefficient is computed by

$$\Gamma(Z_A) = \frac{Z_A - Z_L^*}{Z_A + Z_L} \tag{7}$$

where Z_A is the input impedance of the antenna. We evaluate the antenna impedance and radiation characteristics by full-wave simulation via Ansoft HFSS. The simulated return loss of the three antennas is shown in Fig. 14(a). More specifically, the input impedances are $7.4 + j170.2\ \Omega$ for the proposed inductively coupled-feed antenna, $12.4 + j168.5\ \Omega$ for the patch antenna, and $11.1 + j168.3\ \Omega$ for the quasi-Yagi antenna. All the antennas exhibit good impedance matching; especially, the proposed antenna has a largest bandwidth.

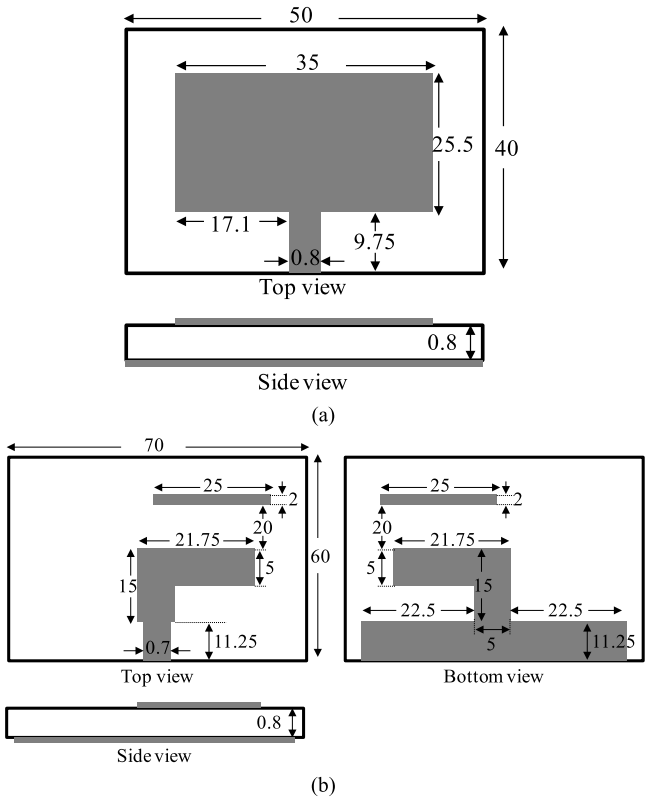

Fig. 13. Configuration of reference rectenna designs. (a) Patch antenna and (b) quasi-Yagi antenna (unit: mm).

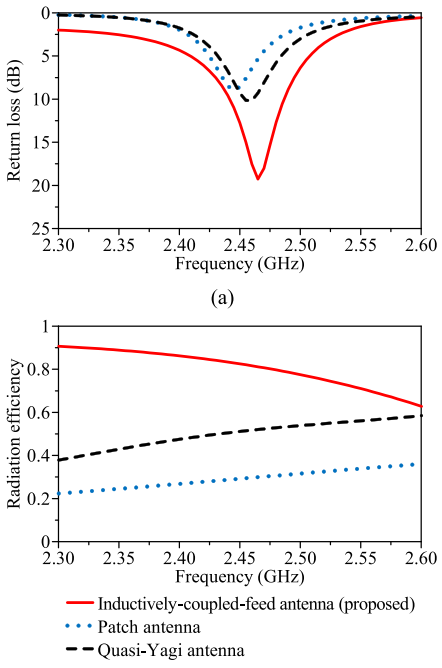

Fig. 14. Comparison of antenna performances between the proposed antenna and the conventional structures. (a) Return loss. (b) Radiation efficiency.

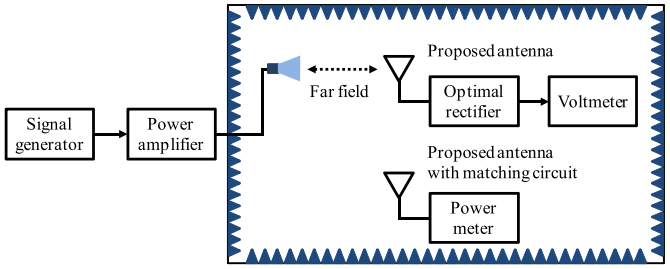

Fig. 15. Experimental setup for the performance evaluation of rectennas.

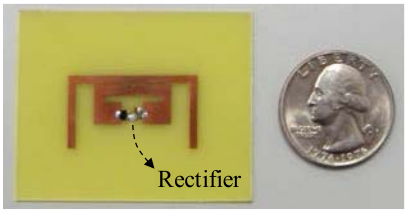

Fig. 16. Photograph of the prototype of the proposed optimized rectenna structure.

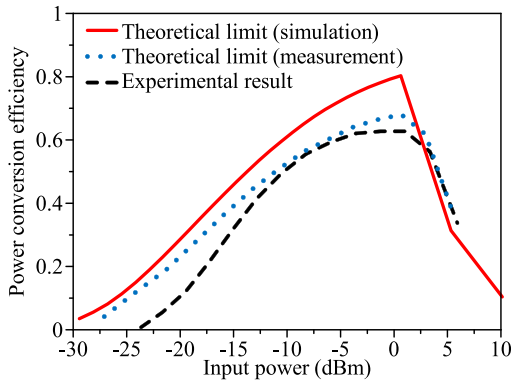

Fig. 17. Comparison of PCE between the efficiency resulting from the proposed structure and the theoretical limit.

However, as the radiation capability is further compared, the radiation efficiency of the proposed antenna is much larger than that of the conventional antennas. The simulated radiation efficiency is shown and compared in Fig. 14(b). The radiation efficiency of the inductively coupled-feed antenna is 82.3%, even though it is printed on a relatively lossy substrate. In contrast, the radiation efficiency of the patch antenna and that of the quasi-Yagi antenna are only 29% and 50.9%, respectively. Although using comparatively lossless substrates such as RO 5880 may enhance the radiation efficiency, the costs are much higher, too. Accordingly, the inductively coupled-feed antenna is very suitable for the purpose of directly conjugate match.

B. Experimental Verification

Next, the proposed optimized rectenna structure, which uses the inductively coupled-feed antenna directly matched to the optimal half-wave rectifier, is tested experimentally. The schematic representation of experimental setup is shown in Fig. 15. The measurement is performed in an anechoic chamber. A microwave signal is generated at 2.45 GHz and boosted from a power amplifier (AR RF/Microwave Instrumentation Model 5S1G4) for sufficient radiating power.

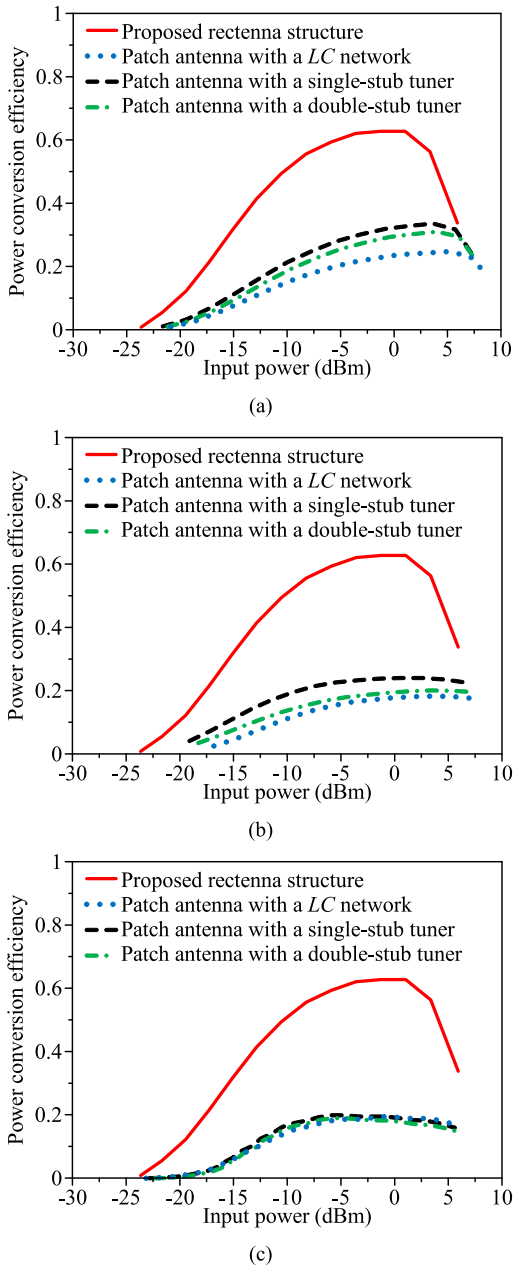

Fig. 18. Measured PCE of rectennas using different energy-harvesting circuits. (a) Half-wave rectifier. (b) Single-stage voltage multiplier. (c) Dickson charge pump.

A standard horn antenna is utilized to transmit 2.45-GHz power. Such power is first measured through a power meter (Keysight technologies U2001A) connected to the proposed antenna, placed in a fixed position. Afterward, the antenna is replaced by the proposed rectenna in the same position. A photograph of the test piece is shown in Fig. 16. By measuring the dc power, the overall PCE can be thus determined.

The measured PCE of the optimized rectenna structure is shown in Fig. 17. It is observed that the peak PCE, 62.9%, occurs when the input power is −1.3 dBm. When the input power is reduced to −15 dBm, the PCE still remains 31.8%. To demonstrate the optimality of the proposed rectenna more clearly, we mark the theoretical limit of PCE derived in

Section II on Fig. 17. Clearly, the PCE of the optimized rectenna structure gets as close as possible to the theoretical limit. Such measured PCE evaluates the overall result, instead of only the rectifier conversion efficiency described in Section II, yet the PCE still follows the upper bound very closely.

To further verify the capability of the proposed rectenna, some rectenna structures operating at 2.45 GHz are fabricated as the reference designs. The receiving element of these reference designs is a patch antenna, the input impedance of which is designed to 50 Ω. The patch antenna is connected to various energy-harvesting circuits, representing regular rectennas in the literature. These energy-harvesting circuits consist of different matching networks (*LC* networks, single-stub tuners, and double-stub tuners) and rectifier topologies (half-wave rectifiers, single-stage voltage multipliers, and Dickson charge pumps), all fabricated on FR4. The return loss of these energy-harvesting circuits has been maximized, and the rectifier parameters have also been optimized to attain the locally maximum PCE. The associated measured results are shown in Fig. 18. Clearly, the proposed rectenna obtains the maximum PCE, whatever the reference designs are being compared. For these reference designs, the largest PCE is only 32.1% at 0 dBm, obtained by the patch antenna connected to the single-stub tuner and the half-wave rectifier. These observations validate the design guidelines presented in this paper, confirming that the proposed rectenna design yields greater PCE.

V. Conclusion

In this paper, we have determined the performance limit of rectennas for the input power ranging from −20 to 0 dBm, and we have achieved such a performance limit by the optimized rectenna structure, which eliminates the matching circuit and exhibits the optimal rectifier architecture. The upper bound of PCE is determined by solving the associated mathematical programming problem, and the results are also validated by numerical optimization and experimental verification. Using the theoretical upper bound, we have compared experimental performance data from a large body of published designs, establishing several important guidelines for rectenna development applying to RF energy harvesting: 1) the maximum PCE is obtained only if all the design factors including operational frequency, rectifier topology, and rectifier parameters are optimized; 2) the matching circuit between an antenna and a rectifier must be eliminated in low-input-power conditions; while no studies have derived the lossyness of matching circuits as the function of input power, we have demonstrated that up to 95% of power may be despoiled even though good impedance matching is established; and 3) instead of patch antennas, which are widely used as the antenna element for RF energy harvesting, the optimal antenna configuration directly matched to the rectifier impedance is the structure with an inductively coupled-feed loop.

Following these design guidelines, we have finally proposed the optimized rectenna structure closely approaching the maximum achievable PCE. This rectenna is designed to operate at 2.45 GHz, and the rectifier circuit is a half-wave rectifier with the optimal load; meanwhile, the matching circuit is eliminated, and the antenna, configured as an inductively coupled-feed dipole, is directly matched to the input impedance of the rectifier. The measured PCE exhibited 61.4%, 50.7%, and 31.8% at $P_{\text{in}} = -5$ dBm, $P_{\text{in}} = -10$ dBm, and $P_{\text{in}} = -15$ dBm, respectively; these results outperform the PCE reported in earlier studies, thereby validating the established design guidelines. It is expected that this will provide useful directions for future rectenna development aiming at low-input-power scenarios.

Acknowledgment

The authors would like to thank Dr. Jui-Hung Chou for his valuable suggestions and technical assistance.

References

[1] V. T. Nguyen, S. H. Kang, J. H. Choi, and C. W. Jung, "Magnetic resonance wireless power transfer using three-coil system with single planar receiver for laptop applications," *IEEE Trans. Consum. Electron.*, vol. 61, no. 2, pp. 160–166, May 2015.

[2] C. R. Valenta and G. D. Durgin, "Harvesting wireless power: Survey of energy-harvester conversion efficiency in far-field, wireless power transfer systems," *IEEE Microw. Mag.*, vol. 15, no. 4, pp. 108–120, Jun. 2014.

[3] T.-W. Yoo and K. Chang, "Theoretical and experimental development of 10 and 35 GHz rectennas," *IEEE Trans. Microw. Theory Techn.*, vol. 40, no. 6, pp. 1259–1266, Jun. 1992.

[4] C. Song *et al.*, "A high-efficiency broadband rectenna for ambient wireless energy harvesting," *IEEE Trans. Antennas Propag.*, vol. 63, no. 8, pp. 3486–3495, Aug. 2015.

[5] H. Sun, Y.-X. Guo, M. He, and Z. Zhong, "A dual-band rectenna using broadband yagi antenna array for ambient RF power harvesting," *IEEE Antennas Wireless Propag. Lett.*, vol. 12, pp. 918–921, 2013.

[6] F. Zhang, F.-Y. Meng, J.-C. Lee, and Q. Wu, "Study of a novel compact rectenna for wireless energy harvesting," in *Proc. IEEE Int. Wireless Symp.*, Beijing, China, Apr. 2013, pp. 1–4.

[7] F. Congedo, G. Monti, L. Tarricone, and V. Bella, "A 2.45-GHz Vivaldi rectenna for the remote activation of an end device radio node," *IEEE Sensors J.*, vol. 33, no. 9, pp. 3454–3461, Sep. 2013.

[8] M. J. Nie, X. X. Yang, G. N. Tan, and B. Han, "A compact 2.45-GHz broadband rectenna using grounded coplanar waveguide," *IEEE Antennas Wireless Propag. Lett.*, vol. 14, pp. 986–989, Dec. 2015.

[9] M. Arrawatia, M. S. Baghini, and G. Kumar, "Broadband bent triangular omnidirectional antenna for RF energy harvesting," *IEEE Antennas Wireless Propag. Lett.*, vol. 15, pp. 36–39, 2016.

[10] S. D. Assimonis, S.-N. Daskalakis, and A. Bletsas, "Sensitive and efficient RF harvesting supply for batteryless backscatter sensor networks," *IEEE Trans. Microw. Theory Techn.*, vol. 64, no. 4, pp. 1327–1338, Apr. 2015.

[11] J. A. Hagerty, F. B. Helmbrecht, W. H. McCalpin, R. Zane, and Z. B. Popovic, "Recycling ambient microwave energy with broad-band rectenna arrays," *IEEE Trans. Microw. Theory Techn.*, vol. 52, no. 3, pp. 1014–1024, Mar. 2004.

[12] V. Kuhn, C. Lahuec, F. Seguin, and C. Person, "A multi-band stacked RF energy harvester with RF-to-DC efficiency up to 84%," *IEEE Trans. Microw. Theory Techn.*, vol. 63, no. 5, pp. 1768–1778, May 2015.

[13] K. Niotaki *et al.*, "A compact dual-band rectenna using slot-loaded dual band folded dipole antenna," *IEEE Antennas Wireless Propag. Lett.*, vol. 12, pp. 1634–1637, 2013.

[14] R. Scheeler, S. Korhummel, and Z. Popovic, "A dual-frequency ultralow-power efficient 0.5-G rectenna," *IEEE Microw. Mag.*, vol. 15, no. 1, pp. 109–114, Jan. 2014.

[15] P. Lu, X. S. Yang, J. L. Li, and B. Z. Wang, "A compact frequency reconfigurable rectenna for 5.2- and 5.8-GHz wireless power transmission," *IEEE Trans. Power Electron.*, vol. 30, no. 11, pp. 6006–6010, Nov. 2015.

[16] F.-J. Huang, C.-M. Lee, C.-L. Chang, L.-K. Chen, T.-C. Yo, and C.-H. Luo, "Rectenna application of miniaturized implantable antenna design for triple-band biotelemetry communication," *IEEE Trans. Antennas Propag.*, vol. 59, no. 7, pp. 2646–2653, Jul. 2011.

[17] Y.-H. Suh and K. Chang, "A high-efficiency dual-frequency rectenna for 2.45- and 5.8-GHz wireless power transmission," *IEEE Trans. Microw. Theory Techn.*, vol. 50, no. 7, pp. 1784–1789, Jul. 2002.

[18] J. Heikkinen and M. Kivikoski, "A novel dual-frequency circularly polarized rectenna," *IEEE Antennas Wireless Propag. Lett.*, vol. 2, no. 1, pp. 330–333, 2003.

[19] D. Masotti, A. Costanzo, M. D. Prete, and V. Rizzoli, "Genetic-based design of a tetra-band high-efficiency radio-frequency energy system," *IET Microw. Antennas Propag.*, vol. 7, no. 15, pp. 1254–1263, Dec. 2013.

[20] M. Pinuela, P. D. Mitcheson, and S. Lucyszyn, "Ambient RF energy harvesting in urban and semi–urban environments," *IEEE Trans. Microw. Theory Techn.*, vol. 61, no. 7, pp. 2715–2726, Jul. 2013.

[21] B. Li, X. Shao, N. Shahshahan, N. Goldsman, T. Salter, and G. M. Metze, "An antenna co-design dual band RF energy harvester," *IEEE Trans. Circuits Syst. I, Reg. Papers*, vol. 60, no. 12, pp. 3256–3266, Dec. 2013.

[22] D. Pavone, A. Buonanno, M. D'Urso, and F. G. Corte, "Design considerations for radio frequency energy harvesting devices," *Prog. Electromagn. Res. B*, vol. 45, pp. 19–35, Jan. 2012.

[23] A. Costanzo, A. Romani, D. Masotti, N. Arbizzani, and V. Rizzoli, "RF/baseband co-design of switching receivers for multiband microwave energy harvesting," *Sens. Actuators A, Phys.*, vol. 179, pp. 158–168, Jun. 2012.

[24] B. L. Pham and A.-V. Pham, "Triple bands antenna and high efficiency rectifier design for RF energy harvesting at 900, 1900, and 2400 MHz," in *Proc. IEEE MTT-S Int. Microw. Symp.*, Seattle, WA, USA, Jun. 2013, pp. 1–3.

[25] V. Rizzoli, G. Bichicchi, A. Costanzo, F. Donzelli, and D. Masotti, "CAD of multi-resonator rectenna for micro-power generation," in *Proc. Eur. Microw. Conf.*, Rome, Italy, Sep. 2009, pp. 1684–1687.

[26] H. Sun, Y.-X. Guo, M. He, and Z. Zhong, "Design of a high-efficiency 2.45-GHz rectenna for low-input-power energy harvesting," *IEEE Antennas Wireless Propag. Lett.*, vol. 11, pp. 929–932, 2012.

[27] A. Georgiadis, G. V. Andia, and A. Collado, "Rectenna design and optimization using reciprocity theory and harmonic balance analysis for electromagnetic (EM) energy harvesting," *IEEE Antennas Wireless Propag. Lett.*, vol. 9, pp. 444–446, May 2010.

[28] X. X. Yang, C. Jiang, A. Z. Elsherbeni, F. Yang, and Y. Q. Wang, "A novel compact printed rectenna for data communication systems," *IEEE Trans. Antennas Propag.*, vol. 61, no. 5, pp. 2532–2539, May 2013.

[29] H. Takhedmit, L. Cirio, S. Bellal, D. Delcroix, and O. Picon, "Compact and efficient 2.45 GHz circularly polarised shorted ring-slot rectenna," *Electron. Lett.*, vol. 48, no. 5, pp. 253–254, Mar. 2012.

[30] B. Strassner and K. Chang, "Highly efficient C-band circularly polarized rectifying antenna array for wireless microwave power transmission," *IEEE Trans. Antennas Propag.*, vol. 51, no. 6, pp. 1347–1356, Jun. 2003.

[31] Y.-J. Ren and K. Chang, "5.8-GHz circularly polarized dual-diode rectenna and rectenna array for microwave power transmission," *IEEE Trans. Microw. Theory Techn.*, vol. 54, no. 4, pp. 1495–1502, Jun. 2006.

[32] F. J. Huang, T. C. Yo, C. M. Lee, and C. H. Luo, "Design of circular polarization antenna with harmonic suppression for rectenna application," *IEEE Antennas Wireless Propag. Lett.*, vol. 11, pp. 592–595, 2012.

[33] Z. Harouni, L. Cirio, L. Osman, A. Gharsallah, S. Member, and O. Picon, "A dual circularly polarized 2.45-GHz rectenna for wireless power transmission," *IEEE Antennas Wireless Propag. Lett.*, vol. 10, pp. 306–309, 2011.

[34] W. Haboubi *et al.*, "An efficient dual-circularly polarized rectenna for RF energy harvesting in the 2.45 GHz ISM band," *Prog. Electromagn. Res.*, vol. 148, pp. 31–39, Dec. 2014.

[35] J.-H. Chou, D.-B. Lin, K.-L. Weng, and H.-J. Li, "All polarization receiving rectenna with harmonic rejection property for wireless power transmission," *IEEE Trans. Antennas Propag.*, vol. 62, no. 10, pp. 5242–5249, Oct. 2014.

[36] H. Sun and W. Geyi, "A new rectenna with all-polarization-receiving capability for wireless power transmission," *IEEE Antennas Wireless Propag. Lett.*, vol. 15, pp. 814–817, 2016.

[37] H. Sun, "An enhanced rectenna using differentially-fed rectifier for wireless power transmission," *IEEE Antennas Wireless Propag. Lett.*, vol. 15, pp. 32–35, 2016.

[38] C. H. K. Chin, Q. Xue, and C. H. Chan, "Design of a 5.8-GHz rectenna incorporating a new patch antenna," *IEEE Antennas Wireless Propag. Lett.*, vol. 4, pp. 175–178, 2005.

[39] A. Collado and A. Georgiadis, "Conformal hybrid solar and electromagnetic (EM) energy harvesting rectenna," *IEEE Trans. Circuits Syst. I, Reg. Papers*, vol. 60, no. 8, pp. 2225–2234, Aug. 2013.

[40] K. Niotaki, F. Giuppi, A. Georgiadis, and A. Collado, "Solar/EM energy harvester for autonomous operation of a monitoring sensor platform," *Wireless Power Transf.*, vol. 1, no. 1, pp. 44–50, Mar. 2014.

[41] H. Takhedmit, L. Cirio, F. Costa, and O. Picon, "Transparent rectenna and rectenna array for RF energy harvesting at 2.45 GHz," in *Proc. Eur. Microw. Conf.*, Hauge, The Netherlands, Apr. 2014, pp. 2970–2972.

[42] U. Olgun, C.-C. Chen, and J. L. Volakis, "Investigation of rectenna array configurations for enhanced RF power harvesting," *IEEE Antenna Wireless Propag. Lett.*, vol. 10, pp. 262–265, 2011.

[43] J. A. C. Theeuwes, H. J. Visser, M. C. van Beurden, and G. J. N. Doodeman, "Efficient, compact, wireless battery design," in *Proc. Eur. Microw. Conf.*, Munich, Germany, Oct. 2007, pp. 991–994.

[44] P. Nintanavongsa *et al.*, "Design optimization and implementation for RF energy harvesting circuits," *IEEE J. Emerg. Sel. Topics Circuits Syst.*, vol. 2, no. 1, pp. 24–33, Mar. 2012.

[45] YU. Ushijima, T. Sakamoto, E. Nishiyama, M. Aikawa, and I. Toyoda, "5.8-GHz integrated differential rectenna unit using both-sided MIC technology with design flexibility," *IEEE Trans. Antennas Propag.*, vol. 61, no. 6, pp. 3357–3360, Jun. 2013.

[46] U. Olgun, C.-C. Chen, and J. L. Volakis, "Design of an efficient ambient WiFi energy harvesting system," *IET Microw., Antennas Propag.*, vol. 6, no. 11, pp. 1200–1206, Aug. 2012.

[47] T. Sakamoto, Y. Ushijima, E. Nishiyama, M. Aikawa, and I. Toyoda, "5.8-GHz series/parallel connected rectenna array using expandable differential rectenna units," *IEEE Trans. Antennas Propag.*, vol. 61, no. 9, pp. 4872–4875, Sep. 2013.

[48] J. Zbitou, M. Latrach, and S. Toutain, "Hybrid rectenna and monolithic integrated zero-bias microwave rectifier," *IEEE Trans. Microw. Theory Techn.*, vol. 54, no. 1, pp. 147–152, Jan. 2006.

[49] K. Nishida *et al.*, "5.8 GHz high sensitivity rectenna array," in *IEEE MTT-S Int. Microw. Symp. Dig. Workshop*, Kyoto, Japan, May 2011, pp. 19–22.

[50] A. Collado and A. Georgiadis, "Optimal waveforms for efficient wireless power transmission," *IEEE Microw. Wireless Compon. Lett.*, vol. 24, no. 5, pp. 354–356, May 2014.

[51] C. R. Valenta, M. M. Morys, and G. D. Durgin, "Theoretical energy-conversion efficiency for energy-harvesting circuits under power-optimized waveform excitation," *IEEE Trans. Microw. Theory Techn.*, vol. 63, no. 5, pp. 1758–1767, May 2015.

[52] M. Roberg, T. Reveyrand, I. Ramos, E. A. Falkenstein, and Z. Popovic, "High-efficiency harmonically terminated diode and transistor rectifiers," *IEEE Trans. Microw. Theory Techn.*, vol. 60, no. 12, pp. 4043–4052, Dec. 2012.

[53] S. Hemour *et al.*, "Towards low-power high-efficiency RF and microwave energy harvesting," *IEEE Trans. Microw. Theory Techn.*, vol. 62, no. 4, pp. 965–976, Apr. 2014.

[54] V. Marian, C. Vollaire, J. Verdier, and B. Allard, "Potentials of an adaptive rectenna circuit," *IEEE Antennas Wireless Propag. Lett.*, vol. 10, pp. 1393–1396, 2011.

[55] K. Niotaki, A. Georgiadis, A. Collado, and J. S. Vardakas, "Dual-band resistance compression networks for improved rectifier performance," *IEEE Trans. Microw. Theory Techn.*, vol. 62, no. 12, pp. 3512–3521, Dec. 2014.

[56] T. Paing, E. Falkenstein, R. Zane, and Z. Popovic, "Custom IC for ultra-low power RF energy scavenging," *IEEE Trans. Power Electron.*, vol. 26, no. 6, pp. 1620–1626, Jun. 2011.

[57] D. Masotti, A. Costanzo, P. Francia, M. Filippi, and A. Romani, "A load-modulated rectifier for RF micropower harvesting with start-up strategies," *IEEE Trans. Microw. Theory Techn.*, vol. 62, no. 4, pp. 994–1004, Apr. 2014.

[58] A. Boaventura, A. Collado, N. B. Carvalho, and A. Georgiadis, "Optimum behavior: Wireless power transmission system design through behavioral models and efficient synthesis techniques," *IEEE Microw. Mag.*, vol. 14, no. 2, pp. 26–35, Mar. 2013.

[59] M. K. Hosain and A. Z. Kouzani, "Design and analysis of efficient rectifiers for wireless power harvesting in DBS devices," in *Proc. 8th IEEE Conf. Ind. Electron. Appl.*, Melbourne, VIC, Australia, Jun. 2013, pp. 651–655.

[60] E. Falkenstein, M. Roberg, and Z. Popovic, "Low-power wireless power delivery," *IEEE Trans. Microw. Theory Techn.*, vol. 60, no. 7, pp. 2277–2286, Jul. 2012.

[61] H.-D. Lang, A. Ludwig, and C. D. Sarris, "Convex optimization of wireless power transfer systems with multiple transmitters," *IEEE Trans. Antennas Propag.*, vol. 62, no. 9, pp. 4623–4636, Sep. 2014.
[62] M. Zargham and P. G. Gulak, "Maximum achievable efficiency in near-field coupled power-transfer systems," *IEEE Trans. Biomed. Circuits Syst.*, vol. 6, no. 3, pp. 228–245, Jun. 2012.
[63] I. Yoon and H. Ling, "Investigation of near-field wireless power transfer under multiple transmitters," *IEEE Antennas Wireless Propag. Lett.*, vol. 10, pp. 662–665, 2011.
[64] J. A. G. Akkermans, M. C. V. Beurden, G. J. N. Doodeman, and H. J. Visser, "Analytical models for low-power rectenna design," *IEEE Antennas Wireless Propag. Lett.*, vol. 4, pp. 187–190, 2005.
[65] J.-Y. Park, S.-M. Han, and T. Itoh, "A rectenna design with harmonic-rejecting circular-sector antenna," *IEEE Antennas Wireless Propag. Lett.*, vol. 3, no. 1, pp. 52–54, Dec. 2004.
[66] H. Takhedmit *et al.*, "Efficient 2.45 GHz rectenna design including harmonic rejecting rectifier device," *Electron. Lett.*, vol. 46, no. 12, pp. 811–812, Jun. 2010.
[67] E. Hairer, G. Wanner, and S. P. Nørsett, *Solving Ordinary Differential Equations I*. Berling, Germany: Springer-Verlag, 1993.
[68] J. A. Ferland and D. Costa, "Heuristic search methods for combinatorial programming problems," Univ. Montréal, Québec, QC, Canada, Tech. Rep. DIRO-1193, Mar. 2001.
[69] H. Eriksson and R. W. Waugh, "A temperature compensated linear diode detector," Design Tip, Agilent Technol., Palo Alto, CA, USA, Tech. Rep., 2000.
[70] D. M. Pozar, *Microwave Engineering*. 3rd ed. New York, NY, USA: Wiley, 2005.
[71] H.-W. Son and C.-S. Pyo, "Design of RFID tag antennas using an inductively coupled feed," *Electron. Lett.*, vol. 41, no. 18, pp. 994–996, Sep. 2005.

Yen-Sheng Chen (M'13) was born in Taichung, Taiwan, in 1985. He received the B.S. degree in electrical engineering and the M.S. and Ph.D. degrees in communication engineering from National Taiwan University, Taipei, Taiwan, in 2007, 2009, and 2012, respectively.

Since 2013, he has been a Faculty Member with the Department of Electronic Engineering, National Taipei University of Technology, Taipei, where he is currently an Associate Professor. His research interests included wireless power transfer, antenna array failure correction, antennas for body centric communications, multiple-input multiple-output antennas for compact base stations, microwave reconfigurable devices, and multiobjective optimization techniques. His current research interests include RF energy harvesting, antenna arrays, radio frequency identification, and engineering data analysis/mining.

Dr. Chen has served on the editorial/review boards of many technical journals, transactions, proceedings and letters.

Cheng-Wei Chiu was born in New Taipei City, Taiwan, in 1991. He received the B.S. and M.S. degrees in electronic engineering from the National Taipei University of Technology, Taipei, in 2014 and 2016, respectively.

In 2016, he joined ASUSTeK Computer Inc., Taipei, as an RF Design Engineer. His current research interests include RF energy harvesting, antennas, wireless communication, and power management.